



Thermodynamic feasibility and multiobjective optimization of a closed Brayton cycle-based clean cogeneration system

Ehsan Amiri Rad¹ · Edris Tayyeban¹ · Ehsanolah Assareh^{2,5} · Amjad riaz^{2,4} · Siamak Hoseinzadeh³ · Moonyong Lee²

Received: 27 May 2023 / Accepted: 28 September 2023 / Published online: 16 November 2023
© The Author(s) 2023

Abstract

The present research has analyzed the energy and exergy of a combined system of simultaneous power generation and cooling. To provide a comprehensive data sheet of this system, the system has been investigated in the temperature range of 300–800 °C, and 6 working fluids, including air, carbon dioxide, nitrogen, argon, xenon, and helium, have been investigated. The parameters affecting the performance of the system, namely the compressor inlet pressure, the compressor pressure ratio, and the intermediation pressure ratio were investigated. The power produced by the Brayton cycle at a pressure ratio of 5.2 is the highest due to the increase in compressor power consumption and turbine power generation. The results of the parametric study showed that the exergy efficiency of the system has the maximum value at the pressure ratio of 4.73. The results of the parametric study showed that increasing the pressure of the compressor does not have a significant effect on the electricity consumption and the temperature of the working fluid due to the constant pressure ratio. The input energy to the heat exchanger of the absorption chiller decreases with the increase in the Brayton cycle pressure ratio, and as a result, the cooling created by the chiller also decreases. In this method, three objective functions of exergy efficiency, energy efficiency, and total production power are considered as objective functions. The most optimal value of intermediation pressure ratio was obtained after the optimization process of 1.389. Also, the most optimal value of the pressure ratio of high-pressure and low-pressure turbines was reported as 2.563 and 1.845, respectively.

Keywords Closed Brayton cycle · Cogeneration system · Thermodynamics analysis · Multi-objective optimization · Cooling

List of symbols

T	Temperature (°C)	K	The ratio of specific heats
P	Pressure (kPa)	Q	Heat transfer rate (kW)
C_p	Specific heat of air and water at constant pressure ($\text{kJ kg}^{-1} \text{K}^{-1}$)	m	Mass flow rate (kg s^{-1})
W	Power (kW)	Ex	Exergy (kW)
		U	Overall heat transfer coefficient ($\text{kW m}^{-2} \text{K}^{-1}$)
		h	Specific enthalpy (kJ kg^{-1})

Ehsan Amiri Rad, Edris Tayyeban, Ehsanolah Assareh and Amjad riaz have contributed equally to this article as the first authors.

✉ Ehsan Amiri Rad
A.amirirad@hsu.ac.ir

✉ Ehsanolah Assareh
Ehsanolah.assareh@gmail.com

✉ Siamak Hoseinzadeh
siamak.hosseinzadeh@uniroma1.it

✉ Moonyong Lee
mynlee@ynu.ac.kr

² School of Chemical Engineering, Yeungnam University, Gyeongsan 38541, South Korea

³ Department of Planning, Design, and Technology of Architecture, Sapienza University of Rome, 00196 Rome, Italy

⁴ Department of Chemical Engineering, COMSATS University, Islamabad (Lahore Campus), Pakistan

⁵ Department of Mechanical Engineering, Dezful Branch, Islamic Azad University, Dezful, Iran

¹ Department of Mechanical Engineering, Center of Computational Energy, Hakim Sabzevari University, Sabzevar, Iran

Subscripts

ph	Physical
ch	Chemical
ex	Exergy
cv	Control volume
Tur	Turbine
v	Vapor
HP	High-pressure
LP	Low-pressure
Comp	Compressor
out	Outlet
in	Inlet
N	Number

Abbreviations

ORC	Organic Rankine cycle
COP	Coefficient of Performance
GT	Gas turbine
IPR	Intermediation pressure ratio
TOPSIS	Technique for Order of Preference by Similarity to Ideal Solution
MED	Multi-effect desalination
WHR	Waste heat recovery

Greek symbol

η	Efficiency (%)
ρ	Density (kg m^{-3})

Introduction

Nowadays, fossil fuel consumption has increased with an increase in population and the growth of various industries. This, in turn, has increased the emission of various environmental pollutants [1]. To address this issue, researchers seek ways to replace fossil fuels and improve the efficiency of energy-consuming systems. In this regard, there are two major solutions. The first solution is the use of renewable energies [2]. The second solution involves optimizing and increasing the efficiency of existing systems, for which various methods have been presented [2]. Research and experience have shown that multi-generation systems, such as combined cooling, heating, and power systems, can significantly improve efficiency and reduce emissions [3]. In addition, recovering the waste heat in various industries and refineries in order to operate multi-generation systems can greatly increase the efficiency of these systems [4, 5]. The recovered waste heat depends on the quality of the dissipated thermal energy and the energy demand of the system and can be utilized for generating power, cooling, fresh water, etc. [6–8]. A major parameter in the selection of the heat recovery system type is the quality of the dissipated energy, which is influenced by the flow rate and temperature of the

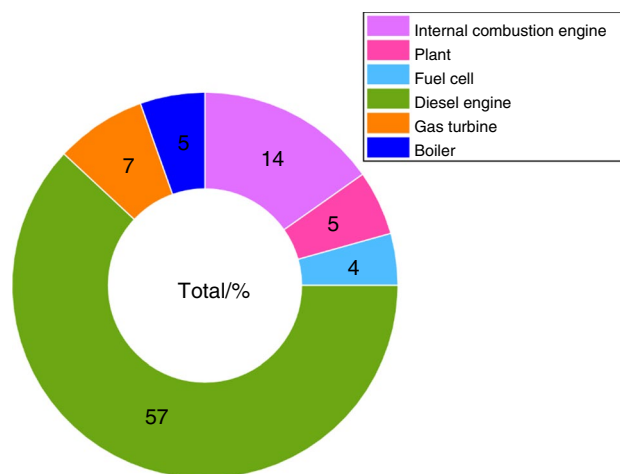


Fig. 1 Percent share of different heat sources used in a WHR system

gas. Figure 1 displays the share of different heat generation sources used in waste heat recovery (WHR) systems [9].

The Brayton cycle can be used up to a temperature of 1000 °C depending on the application and hence, creates good flexibility in selecting the heat source [10]. This cycle can be either open or closed [11]. In an open cycle, the working fluid is air, which provides the energy required by a turbine by burning with fuel [12]. In this case, other gases, such as helium, CO₂, etc. cannot be used as the working fluid. Moreover, due to the discharge of combustion products to the environment, this cycle is not suitable in terms of energy and environmental efficiency. As a result, it is often used in combination with other cycles [13]. On the other hand, the closed Brayton cycle does not discharge the working fluid to the environment and, thus, allows designers to examine different working fluids. However, this cycle also needs additional systems to improve its energy efficiency due to the high temperature of the fluid at the turbine outlet.

To this end, numerous studies have been conducted, and researchers have investigated various hybrid systems. Naserian et al. [14] studied the cycle introduced by Alali and Al-Shaboul [15] and launched a closed Brayton cycle using waste heat from a nuclear reactor. They also used the exhaust gases from the Brayton cycle to produce steam and heating. Four working fluids were studied, namely N₂, He, CO₂, and air. According to their results, He performed best in power generation, while N₂ and air produced a higher specific power. Moreover, CO₂ exhibited superior performance in steam generation (heating system). In another study, Romano and Riberio [16] examined and optimized the cold-side temperature of the Brayton cycle. The cycle they studied transferred the heat from the turbine outlet flow to the pipes via a heat exchanger and further to the environment via radiators for heating purposes. The ratio of the generated power to the surface area of the radiators was considered

the objective function. The results indicated that this ratio was maximum when the temperature of the heat pipes was between 450 and 500 K. Wang et al. [17] tried to combine an internal combustion engine, closed Brayton cycles, refrigeration, and organic Rankine cycle (ORC). Also, in this research, using the single objective optimization method, the compressor inlet temperature and pressure ratio, the Brayton turbine inlet temperature, the ORC turbine inlet pressure and the ejector outlet pressure have been obtained as 3, 36.242 C, 435.404 C, 1.363 MPa, and 1.556 MPa, respectively. Abbasi and Pourrahmani [18] studied a hybrid system consisting of the Brayton cycle, ORC, and an absorption chiller using multi-objective optimization and eco-exergy methods by considering solar energy as a heat source. They employed a (phase change material) PCM tank for using the system at night. As such, the system could work 24 h a day by storing solar energy by the ammonia storage source, during the day and utilizing it at night. Moreover, the reverse osmosis (RO) desalination system was operated by using the power generated by the ORC system. Based on the results, in the optimal state, the pressure ratio of the Brayton cycle compressor, the turbine inlet pressure, the exergy efficiency, and the energy efficiency were 9.06, 3300 kPa, 14.40%, and 40.5%, respectively. Furthermore, the generated amounts of power, cooling, and water were obtained to be, respectively, 2.42 MW, 1.6 MW, and 5209.5 m³/day. In another study, Yongming Feng et al. [19] conducted a thermodynamic and optimization study on a hybrid Brayton-Kalina cycle. In this research, the diesel generator exhaust was considered to be the heat source. According to the results, the annual fuel cost decreased by 16.62%, and the energy efficiency improved by 15.01%. Ahmadi et al. [20] studied the combination of an open Brayton cycle with the ORC and absorption chiller cycles. The system proposed in this research was capable of heating, cooling, and power cogeneration. The results showed that the highest irreversibility and exergy destruction occurred in the combustion chamber and the heat exchanger. Moreover, a study of the emitted CO₂ indicated that emissions of this gas had been reduced due to the simultaneous use of different systems. Extensive research has been carried

out in the field of WHR, the most important of which studied the combination of cycles such as Brayton, ORC, absorption chiller, and desalinations. Some of this research has already been mentioned in Table 1.

In 2020, Liu et al. investigated the Brayton cycle for power generation systems. This study aimed to minimize the total mass of the power system through the optimization of the influencing parameters of the system components. The results showed that increasing the turbine inlet temperature by 4% from the value of 1150 K leads to a 6% reduction in the mass of the system [26]. In 2020, Kim et al. did work on a parametric study and optimization of a closed Brayton cycle considering fluid charging. The results showed that the amount of charge can be considered as a design and control parameter of CBC [27]. In 2020, Zhang et al. investigated a new power generation system using a gas turbine cycle. Based on the optimization results, the thermal and exergy efficiency of the system was reported as 46.11% and 47.24% [28]. In 2022, Musharavati et al. investigated biomass gasification for electricity and freshwater production. The main components of this power plant include a gasifier, a compressor, a heat exchanger, a gas turbine, a combustion chamber, and a multi-effect desalination unit with thermal vapor compression [29]. In 2023, Khanmohammadi et al. investigated an energy-based multigeneration system. The heliostat had the highest exergy destruction rate with 1867 kW. Pump and heliostat units had the lowest exergy efficiency with values of 52.09% and 65.39% [30]. In 2023, Ding et al. evaluated a multiple-generation multi-generation energy system. In this research, a new system consisting of the Kalina cycle, organic Rankine cycle, refrigeration cycle, and electrolyzer was evaluated. The proposed system can produce 80.1 kW and 1930 g/h of electricity and hydrogen fuel, respectively [31]. In 2022, Colakoglu and Durmayaz worked to investigate a new multiple energy generation system based on a solar tower with a triple combined power cycle. Under optimal conditions, the system had energy and exergy efficiency values of 51.99% and 37.99%, respectively, and contributed to 513.8 kg of carbon dioxide emissions reduction per hour [32].

Table 1 Comparative presentation of prior integrated cogeneration systems with respect to power generation, cooling capacity and the maximum temperature

Reference	Technology	Power generation/kW	Cooling capacity/kW	Maximum temperature/°C	Working fluid
Miao et al. [21]	CBC	167.9	–	932–990	S-CO ₂
Sachdeva and Singh. [22]	BC-RC-ORC	331.59	–	1266.63	Air
Abrosimov et al. [23]	IBC-ORC	–	–	600	Exhaust gas (IBC) and R245fa (ORC)
Mohammadi and Amiri rad [24]	RC	5750	–	370	Water
Tayyeban et al. [25]	ORC-REC-MED	187.7	1937	440	R141b

The use of energy systems is necessary to improve consumption and increase the performance of energy systems. With the increase in the world's population, as well as the decrease in fossil resources, and on the other hand, the increase in environmental pollution, more attention should be paid to energy production systems. For this reason, in recent years, many studies have been conducted in the field of increasing the performance of energy production systems with various methods, including heat recovery from the system, optimization, integration of several systems together, simultaneous production, etc. [33–44].

Today, the energy crisis, the increase in greenhouse gas emissions and global warming are critical challenges in the world, especially in developing countries, and the optimal and correct use of energy can be a suitable solution for these problems. For this reason, a lot of research has been done in this field, but more research is needed [45–55].

Nowadays, it is inevitable to implement new power plants with high efficiency to deal with environmental challenges. Because the world's need for energy is increasing day by day, high-capacity systems for production must be set up. One of the most common power generation cycles around the world is the Brayton cycle, which uses natural gas. Energy consumption is one of the appropriate criteria for determining the level of progress and quality of life in a country. Continuity of energy supply and the possibility of long-term access to resources require a comprehensive energy planning and for this reason energy planning is considered an undeniable economic, national and strategic necessity. Energy demand is increasing day by day in the world. Energy has a significant impact on the ability of industries to produce, the type of tools and machines, the methods of exploitation and transportation. Man has become so dependent on energy that he rarely even bothers to think about its role and impact.

Today, meeting energy needs with the least environmental impact is a serious challenge that must be solved with knowledge and technology. Therefore, the development of economic energy systems that provide the maximum use of non-renewable energy sources for electricity production is of great importance. In this regard, in this research, a system for producing clean electricity is proposed to deal with this issue. The need for this system is recommended especially in different climates to meet the need for electrical energy.

The present study examines a multi-generation system for the simultaneous production of electricity and cooling through waste heat. The studied system consists of a closed Brayton cycle whose waste heat is used by an ORC, leading to improved energy efficiency. In addition, excess heat from the exhaust that cannot be used in the Brayton cycle enters the absorption chiller cycle to provide cooling. The purpose of this research is to increase system performance and system productivity.

In short, the current work activity is as follows:

- Introducing a new system of combining Brayton cycle units, organic Rankine cycle with the aim of maximum power generation.
- Using the waste heat of the Brayton cycle to supply the energy required for the Rankine organic cycle.
- Using energy, exergy and exergoeconomic analyzes to provide a comprehensive view of system performance and capabilities.
- Provide a sensitivity analysis to evaluate the impact of design variables on system performance for a deeper understanding of the method.
- Multi-objective optimization of the system to increase the performance of the proposed system.
- Selection of three objective functions of exergy efficiency, energy efficiency and system production power.
- Using the TOPSIS multi-criteria decision making method to find the best and most optimal Pareto point that represents the best performance of the system.

System description

The present research examines the feasibility of using waste heat from the exhaust flare of a refinery via a combination of the closed Brayton cycle, the ORC, and the absorption chiller cycle. Based on the information collected from the refineries in Iran, the flow rate of gas flare varies from 7 to 13 kg s⁻¹. In addition, its temperature can reach 1000 °C. Accordingly, the flow rate of the hot fluid entering the heat exchanger is considered to be 10 kg s⁻¹ for modeling the system and extracting the results. The proposed system is displayed in Fig. 2. In this system, the Brayton cycle consists of two heat exchangers (heater and reheater), high-pressure (HP) and low-pressure (LP) turbines, and a compressor. Moreover, the absorption chiller and the ORCs are of simple types. The working fluid of the Brayton cycle is variable. As can be seen, the exhaust flare first enters the Brayton cycle and loses heat to the working fluid. Then, it transfers part of its energy to the Brayton cycle again by passing through the reheater. Subsequently, cooling is generated as the gas passes through the generator of the absorption chiller cycle. Finally, the gas is discharged from the system at a minimum temperature of 120 °C. In the Brayton cycle, the fluid gains temperature after passing through the compressor and receiving heat in the heat exchanger (this increase in temperature depends on the temperature of the heat source). The fluid enters the first turbine at Point 3, where some of its thermal energy is converted to power. Then, it enters the reheater at Point 4, where its temperature increases at constant pressure. At Point 5, it enters the LP turbine, re-producing power. Given that the fluid must be cooled before entering the compressor, an ORC is used to reduce the temperature of the working

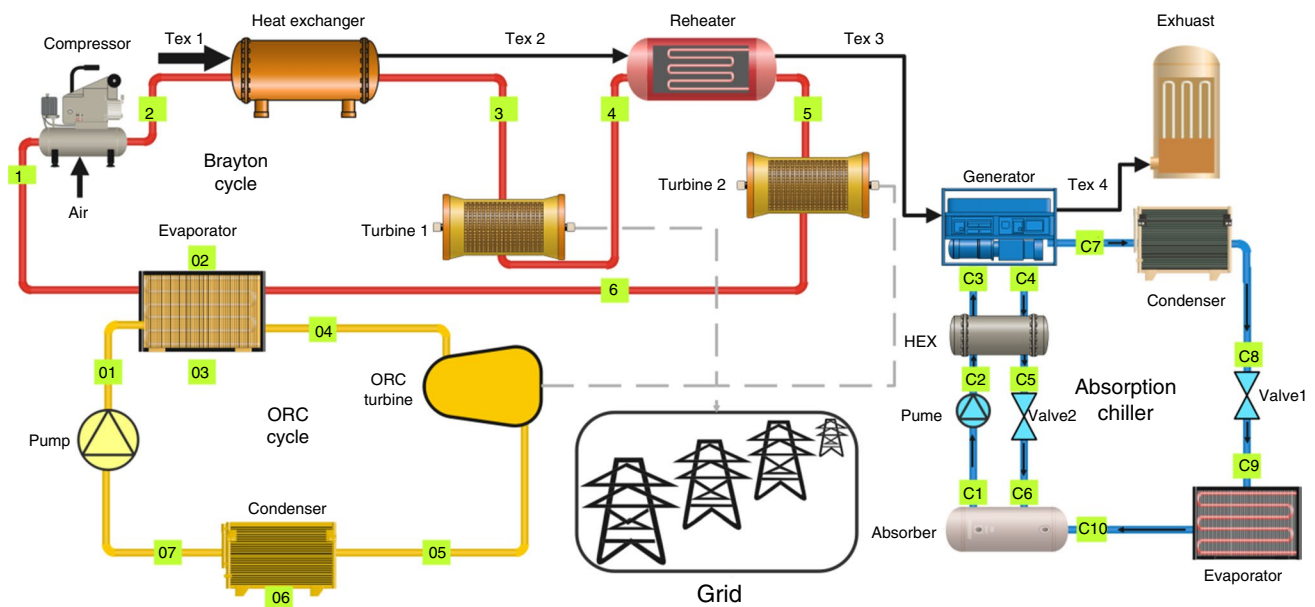


Fig. 2 A schematic of the proposed system

fluid of the Brayton cycle and prevent heat loss. Hence, the temperature of the fluid drops as it exchanges heat with the ORC. This process continues again.

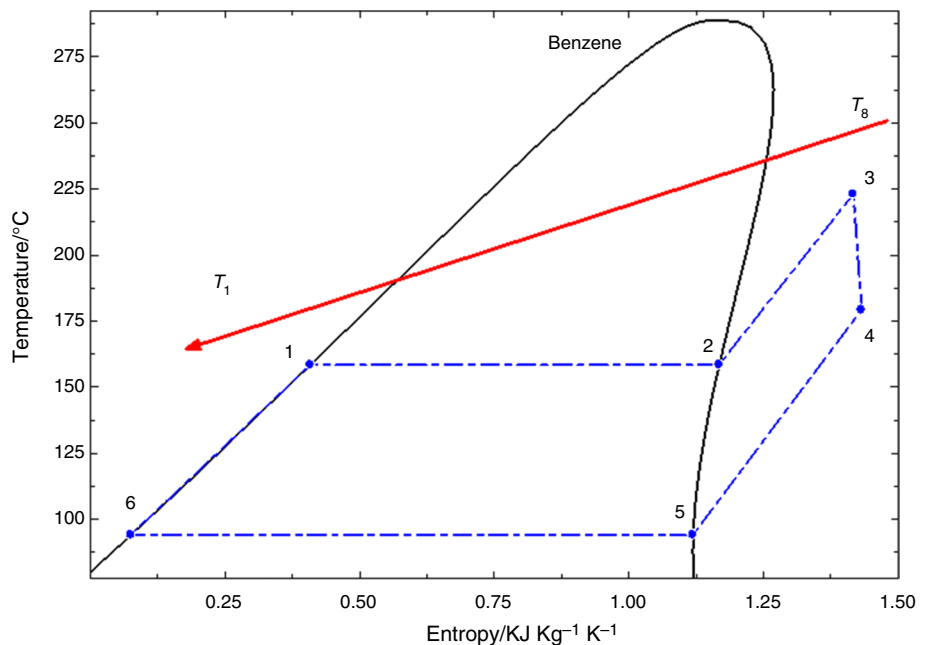
As mentioned previously, the outlet fluid of the LP turbine enters the ORC power generation cycle, where heat is exchanged, leading to a reduction in the temperature of the Brayton cycle fluid before it enters the compressor and generates power, which improves the system performance. Figure 3 displays the T-S graph of the ORC with benzene as the working fluid.

Methodology

This section describes the modeling of the system equipment. To this end, first, the assumptions made for the thermodynamic modeling and analysis are presented. The assumptions are as follows [56, 57]:

- The system operates at a steady-state condition.
- Temperature and pressure heat loss are ignored.

Fig. 3 T-S graph of the ORC with benzene as the working fluid



- Changes in the kinetic and potential energies are ignored for exergy calculations.
- The ambient temperature and pressure are considered to be 25 °C and 101 kPa, respectively.
- Pressure losses in pipelines and heat exchangers can be neglected.
- The isentropic efficiency of compressors, gas turbines, ORC turbines, and pumps are 85, 87, and 90%, respectively.
- Ideal gas mixture law is applied and considered for synthesis gas, fuel and combustion due to high temperatures in gasifier and combustion chamber.

The exhaust gas flow rate is considered to be 10 kg s⁻¹ in this research. Other parameters affecting the design are presented in Table 2.

Closed Brayton cycle

The cycle used in this research is the closed Brayton cycle, which makes use of waste heat. As shown in Fig. 2, this system generates power by absorbing the exhaust heat in two stages (heater and preheater) and using LP and HP turbines. Moreover, the power generated by the turbine and compressor are determined by Eq. (3) and (4), respectively [59, 60].

Table 2 Parameters for designing the multi-generation system [58]

Cycle	Variable	Value	Unit
Exhaust	Mass flow rate	10	kg s ⁻¹
	Pressure	101	kPa
	Input temperature	250–800	°C
Brayton	Working fluid	He, Air, O ₂ , N ₂ , CO ₂ , Xe	–
	Number of compressors	1	
	Compressor efficiency	85	%
	Number of turbines	2	–
	Turbines efficiency	87	%
	Compressor input pressure	101.3	kPa
	Absorption chiller	Working fluid	water + LiBr
ORC	Condenser temperature	35	°C
	Absorption temperature	35	°C
	Evaporation temperature	5	°C
	Pump efficiency	90	%
	SHX effectiveness	0.8	–
	Working fluid		
	Turbines efficiency	90	%
Condenser temperature	35	°C	
Turbine pressure ratio	4.5	–	
Pump efficiency	90	%	

$$Q_{HX1} = m_{wf}(h_4 - h_3) \quad (1)$$

$$Q_{HX2} = m_{wf}(h_6 - h_5) \quad (2)$$

$$W_{Tur_k} = \eta_{Tur} \cdot m_{wf}(\Delta h) \quad (3)$$

$$W_{Comp} = \frac{m_{wf}(\Delta h)}{\eta_{Comp}} \quad (4)$$

In these equations, η_{Comp} and η_{Tur} represent the isentropic efficiency of the compressor and turbine, respectively (Table 2). Also, the following equation is used to compute the cross-sectional area of the heat exchangers [36, 42].

$$A_k = \frac{Q_k}{U_k \cdot \Delta T_{lm_k}} \quad (5)$$

where U_k is the overall heat transfer coefficient. Table 3 presents the overall heat transfer coefficient for all the heat exchangers [61, 62].

ORC unit

Due to the closed nature of the gas cycle, a cooling tower is required to reduce the temperature of the outlet fluid from the second turbine via the exchange of heat. However, this increases the energy losses in the system. Hence, the waste heat from the gas turbine cycle is transferred to the ORC via a heat exchanger by eliminating the cooling tower. In addition, the power consumption of its pump is obtained from Eq. (5) [35, 41, 42].

$$W_{pump} = m_{ORC} \cdot \frac{v_7(P_1 - P_7)}{\eta_p} \quad (6)$$

Table 3 Overall heat transfer coefficient for all the heat exchangers [35–47]

Cycle	Equipment	U/W m ⁻² k
Brayton	Main heat exchanger	937
	Reheater	20
	recuperator	20
ORC	Evaporator	10
	Condenser	10
Absorption chiller	Generator	205
	Condenser	995
	Evaporator	937
	Absorber	696
	Solution heat exchanger	1021

Here, η_{pump} denotes the isentropic efficiency of the pump. Equation (7) is used to calculate this value [35, 41, 42].

$$\eta_{\text{pump}} = \frac{75 + 11.5 \log_{10}(W_p) - 1.5[\log_{10}(W_p)]^2}{100} \quad (7)$$

Absorption chiller

Given the flow rate and temperature of the exhaust after the preheater, it is possible to recover the waste heat. A single-effect absorption chiller was used for this purpose. Moreover, the working fluid is a lithium-bromide/water mixture. As shown in Fig. 2, the thermal energy enters the absorption chiller cycle via a generator. Hence, the maximum temperature occurs in the generator. The fluid entering the generator, which is a mixture of water and lithium, receives heat, part of its water evaporates, and it is divided into two parts: water vapor and a concentrated mixture. The water vapor enters the condenser and is converted to saturated liquid after the exchange of heat (with an external source at a lower temperature). This liquid enters a pressure valve and loses pressure as the temperature decreases to 5 °C at constant enthalpy. This temperature can vary depending on the application. In addition, the concentrated mixture enters the heat exchanger first due to its high temperature and preheats the backflow from the absorber. Then, it passes through the pressure-relief valve, reaches the pressure of the evaporator inlet water, and enters the absorber. In the absorber, water

is reabsorbed by the lithium-bromide mixture. This absorption process is exothermic; hence, heat is exchanged with an external heat source. Equation (8) determines the heat entering the absorption chiller [34, 40, 62].

$$Q_{\text{in generator}} = m_{\text{ex}}(h_{\text{ex}_3} - h_{\text{ex}_4}) = m_{\text{apn}_7}h_{\text{apn}_7} + m_{\text{apn}_3} - m_{\text{apn}_4}h_{\text{apn}_4} \quad (8)$$

The heat transfer surface in the generator, condenser, evaporator, absorber, and solution heat exchangers can be calculated in a similar manner to Eq. (8). The heat transfer coefficients are also shown.

Exergy analysis

Exergy refers to the part of energy that can be used in different forms. Exergy balance was used to calculate the exergy destruction in different equipment. Equation (9) represents the exergy balance [40, 42].

$$EX_{\text{in}_k} - EX_{\text{out}_k} + EX_{\text{destruction}_k} = \frac{\delta EX_k}{\delta t} \quad (9)$$

In this equation, $\frac{\delta EX}{\delta t} = 0$ since steady-state conditions are considered. Table 4 presents the exergy balance for different equipment. Moreover, Eq. (10) is used to compute the exergy efficiency [40, 42].

$$\eta_{\text{ex}} = 1 - \left(\frac{EX_{\text{destruction}}}{EX_{\text{in}}} \right) \quad (10)$$

Table 4 Exergy balance for different component [33–44]

Cycle	Component	Exergy balance equation	
Brayton	Compressor	$EX_1 + W_{\text{in}_c} = EX_2 + EX_{D_c}$	
	Recoperatour	$EX_2 + EX_7 = EX_3 + EX_8 + EX_{D_{pr}}$	
	Heat Exchanger	$EX_3 + EX_{\text{ex}_1} = EX_4 + EX_{\text{ex}_2} + EX_{D_{HX}}$	
	HP turbine	$EX_4 = EX_5 + W_{\text{out}_{HP}} + EX_{D_{HPT}}$	
	Reheater	$EX_5 + EX_{\text{ex}_2} = EX_6 + EX_{\text{ex}_3} + EX_{D_{nr}}$	
	LP turbine	$EX_6 = EX_7 + EX_{D_{LPT}} + W_{\text{out}_{LPT}}$	
ORC	Evaporator	$EX_8 + EX_{\text{orc}_1} = EX_1 + EX_{\text{orc}_4} + EX_{D_{\text{ev}^{\text{orc}}}}$	
	Turbine	$EX_{\text{orc}_4} = EX_{\text{orc}_5} + W_{\text{out}_{\text{orc}}} + EX_{D_{\text{orc}_T}}$	
	Condenser	$EX_{\text{orc}_5} + EX_{\text{cw}_i} = EX_{\text{orc}_7} + EX_{\text{cw}_o} + EX_{\text{orc}_{D_{\text{cdr}}}}$	
	Pump	$EX_{\text{orc}_7} = EX_{\text{orc}_1} + W_{\text{orc}_p} + EX_{D_{\text{orc}_p}}$	
Absorption chiller	Absorber	$EX_{\text{apn}_6} + EX_{\text{apn}_{10}} + EX_{\text{cw}_i} = EX_{\text{apn}_1} + EX_{\text{cw}_o} + EX_{\text{apn}_{D_{\text{abs}}}}$	
	Pump	$EX_{\text{apn}_1} = EX_{\text{apn}_2} + W_{\text{apn}_p} + EX_{\text{apn}_{D_p}}$	
	Expansion valve 1		$EX_{\text{apn}_5} = EX_{\text{apn}_6} + EX_{\text{apn}_{D_{\text{ev}1}}}$
			$EX_{\text{apn}_2} + EX_{\text{apn}_4} = EX_{\text{apn}_3} + EX_{\text{apn}_5} + EX_{\text{apn}_{D_{\text{SHX}}}}$
	Generator	$EX_{\text{apn}_3} + EX_{\text{ex}_3} = EX_{\text{apn}_4} + EX_{\text{apn}_7} + EX_{\text{ex}_4} + EX_{\text{apn}_{D_{\text{gen}}}}$	
	Condenser	$EX_{\text{apn}_7} + EX_{\text{cw}_i} = EX_{\text{apn}_8} + EX_{\text{cw}_o} + EX_{\text{apn}_{D_{\text{cdr}}}}$	
	Expansion valve	$EX_{\text{apn}_8} = EX_{\text{apn}_9} + EX_{\text{apn}_{D_{\text{ev}2}}}$	
	Evaporator	$EX_{\text{apn}_9} + EX_{\text{iw}_i} = EX_{\text{apn}_{10}} + EX_{\text{iw}_o} + EX_{\text{apn}_{D_{\text{eva}}}}$	

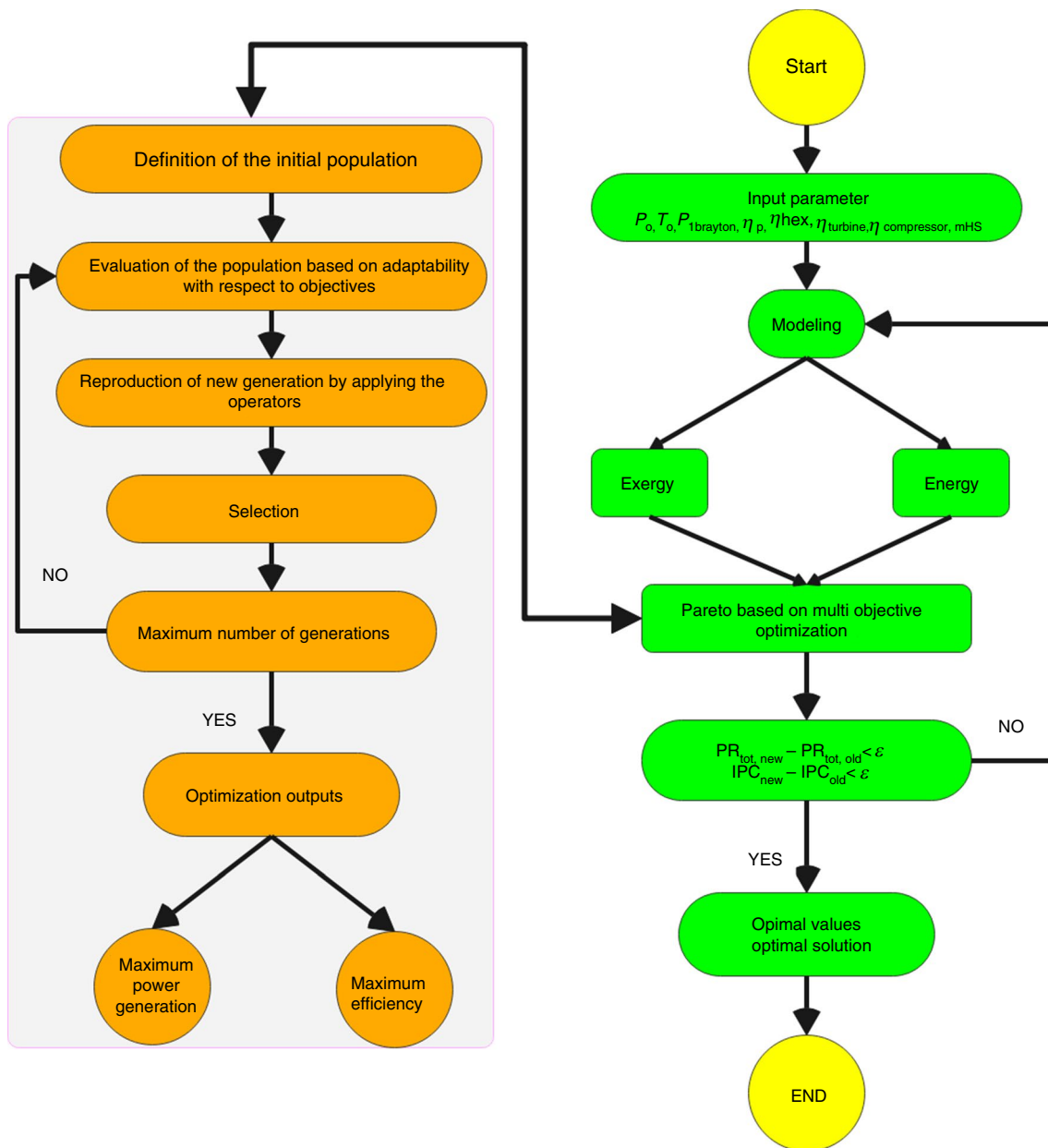


Fig. 4 A schematic of the system modeling and optimization

Coefficient of performance

Coefficient of performance or COP represents the efficiency of absorption chiller cooling devices. The COP performance coefficient is obtained by the ratio of thermal power taken from the air of the desired space or water and any other fluid to the input electrical power or the sum of electrical power and input thermal power. The performance factor is the same as the efficiency of machines, but its value is more than 100%. If its value is less than 100% for a device, that device will not work properly. That's why COP is greater

than 1 or 100%, which, while converting all work into heat, pumps heat from a source to where it is needed, and this COP greater than 1 does not mean that The desired device has an efficiency higher than 100%. Transferring heat from one place to another requires less energy than converting work into heat. The absorption chiller coefficient of performance (COP) is calculated from Eq. 11 [63–67]:

$$\text{COP} = \frac{Q}{W} \quad (11)$$

Table 5 Optimization variables and their range

Name	Lower bound	Upper bound
Compressor pressure ratio	100	1000
Intermediation pressure ratio (IPR)	0.5	3.5

Optimization

Currently, many problems in various fields require optimization and the selection of an optimal point due to the conflict between the behavior of different parameters. The optimal point is selected based on the significance of different parameters, and no single parameter is the sole basis for selection. In this regard, multi-objective optimization methods are widely used in different areas. The Pareto solution method is a suitable multi-objective optimization method with acceptable performance. There are various techniques, such as linear programming technique for multidimensional analysis of preference (LINMEP), Technique for Order of Preference by Similarity to Ideal Solution (TOPSIS), etc. for selecting the optimal point in the Pareto method. The present research used the TOPSIS technique. In this method, the point furthest from the worst point and nearest to the best point is selected as the optimal point.

TOPSIS is a multi-indicator decision-making method for evaluating and prioritizing options based on criteria according to their distance from positive and negative ideals. The

underlying logic of this method defines the ideal solution and the negative ideal solution. The ideal solution is the one that increases the benefit criterion and decreases the cost criterion. The optimal option is the option that has the smallest distance from the ideal solution and at the same time the farthest distance from the negative ideal solution. In the ranking of options by the TOPSIS method, the options that are most similar to the ideal solution are ranked higher. The target space between two criteria is shown as an example in the figure. Here, A+ and A− are the ideal solution and the negative ideal solution, respectively [67, 68].

In this research, compressor pressure ratio and intermediation pressure ratio were considered as decision variables, three target functions of total power generation, energy efficiency and exergy were considered as target functions to improve system performance.

The Pareto diagram is drawn to show the simultaneous optimization of the objective functions and to find the best value of the objective functions. In this research, three objective functions of energy efficiency, exergy efficiency and production power were considered as optimization functions to improve system performance, and the purpose of drawing a three-dimensional optimization diagram, which is called Pareto diagram, is to find the best Pareto point, which it shows the most optimal performance of the system. A Pareto chart is used to highlight the most important factors among a set of factors. This diagram in the quality control process often shows the causes of the most common defects or the reason for the most common customer complaints. After finding a range of optimal

Fig. 5 The effect of the compressor inlet pressure on the total generated work and cooling

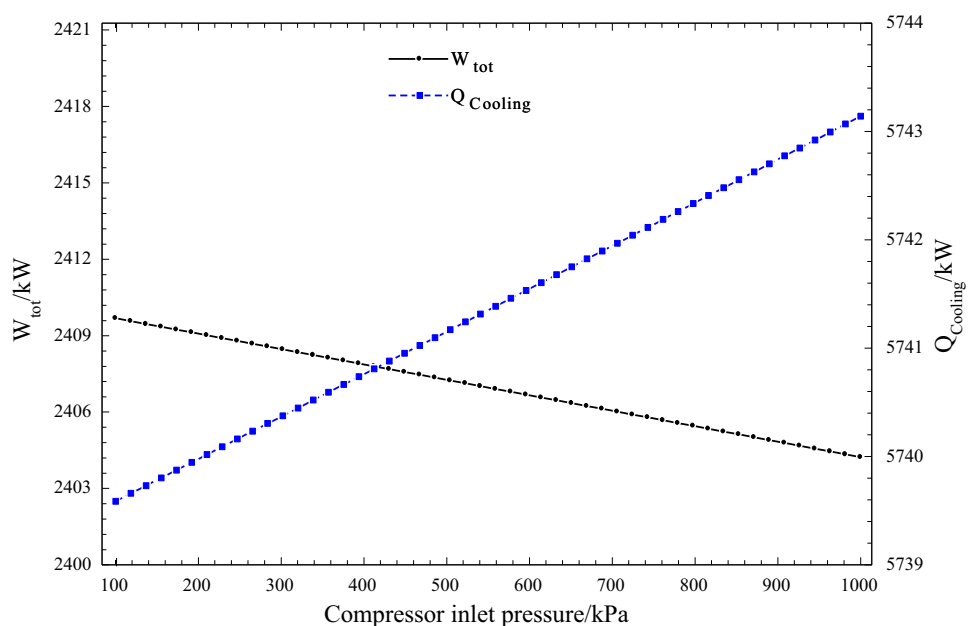
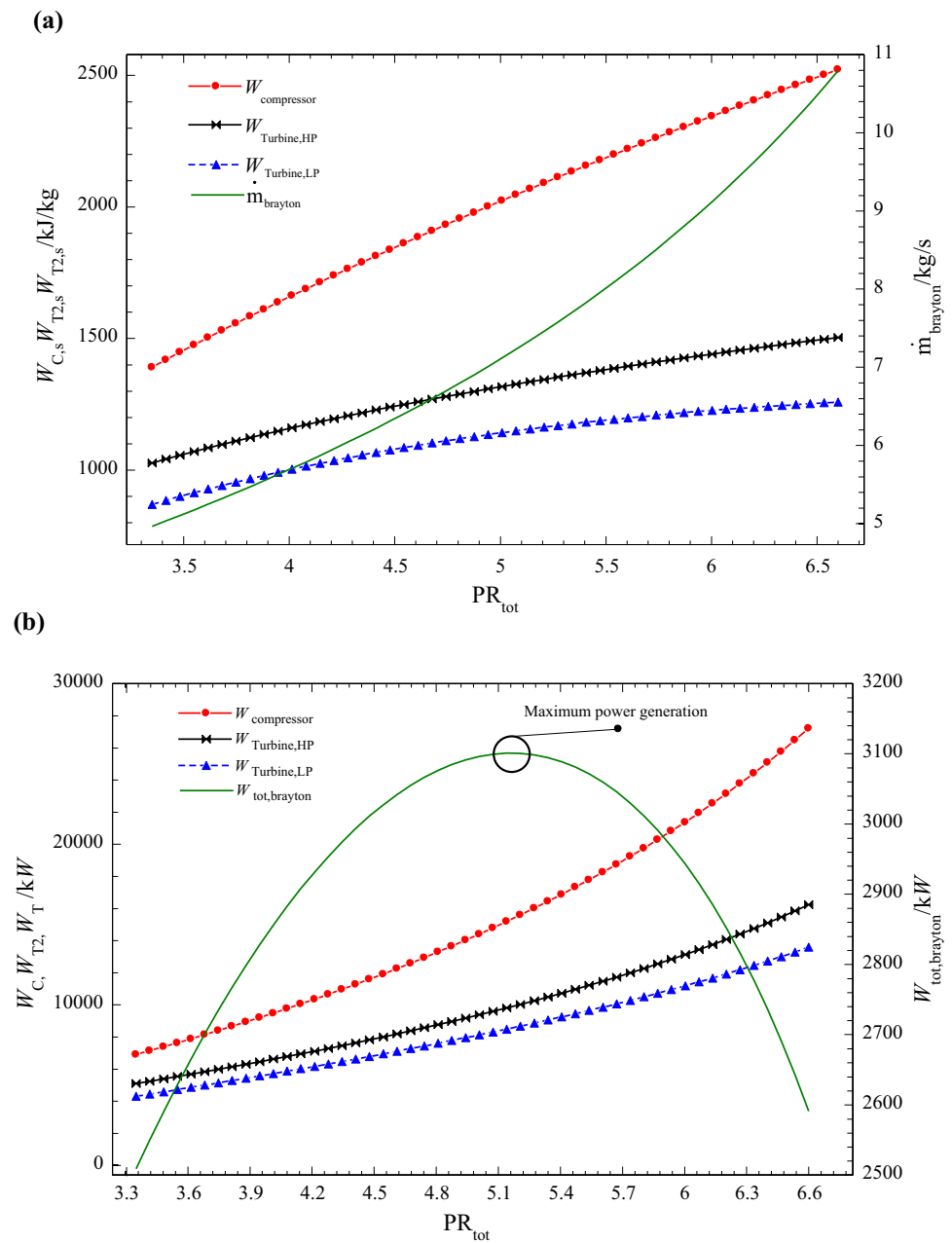


Fig. 6 The effect of an increase in the pressure ratio on **a** the specific work of the compressor and HP and LP turbines and the flow rate in the Brayton cycle and **b** the total power consumption of the compressor and LP and HP turbines and the total work generated by the Brayton cycle



points with the multi-objective optimization method and drawing a Pareto diagram, the TOPSIS method, which is a decision-making method for finding the best and worst points, finds the most optimal Pareto point among different points (Fig. 4).

Table 5 presents the range of decision making variables.

Results and discussion

The variable parameters of the system are inlet pressure and pressure ratios of compressor and turbines in the Brayton cycle, and the maximum pressure of the ORC. Accordingly, these parameters are first examined for helium as the working fluid and a heat source with a temperature of

Fig. 7 The effect of an increase in the pressure ratio on the energy absorbed in the reheater and the absorption chiller

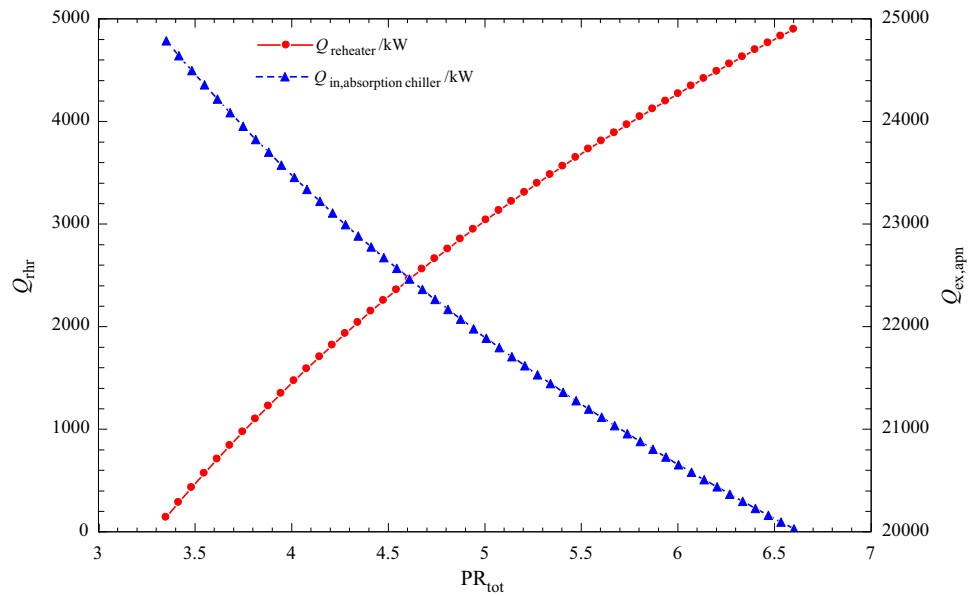
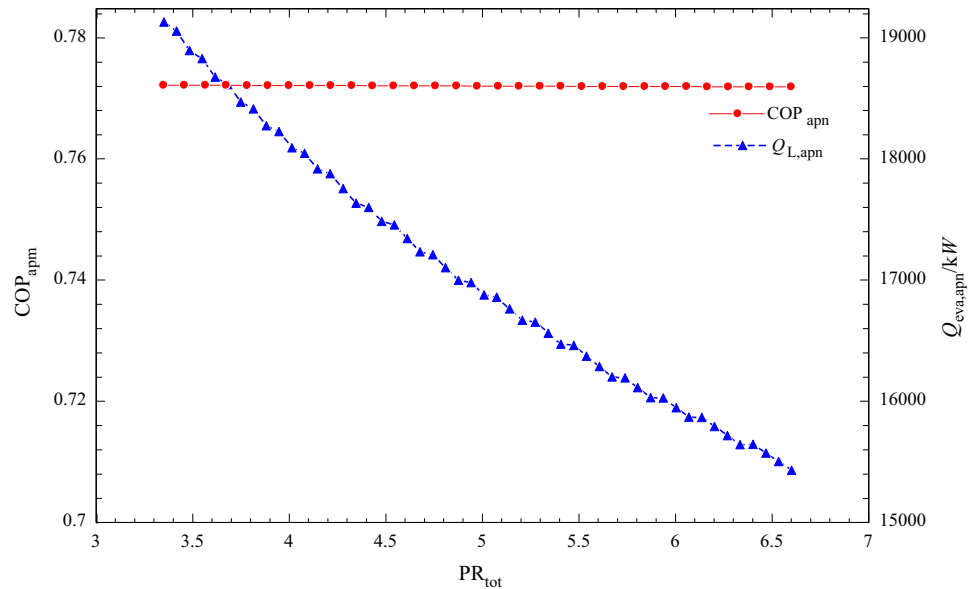


Fig. 8 The effect of an increase in the pressure ratio on the cooling generation and the COP of the absorption chiller



800 °C. Subsequently, the effects of these parameters on the power and cooling generation are investigated, and the optimal value of each parameter is determined. In the first step, the objective is to select an optimal compressor inlet pressure. A rise in the compressor’s pressure does not significantly affect its power consumption and the working fluid’s temperature due to its pressure ratio being constant. Hence, the variations in the system due to an increase in the inlet pressure of the Brayton cycle are negligible. Figure 5 shows the effect of the compressor inlet pressure on the total generated work and cooling. As seen in the figure,

increasing the compressor pressure ratio from 100 to 1000 has reduced the total power of the system from 2409.5 to 2403.5 kW, which has caused a 0.24% reduction in the system’s production power rate, which is very small and insignificant. Also, the results show that the increase in the compressor pressure ratio from 100 to 1000 has caused an increase in the production rate of the system from 5739.8 to 5743.2 kW, which has caused a 0.059% increase in the production cooling rate of the system, which is considered very little. Thus, the initial pressure was considered to be 100 kPa.

Fig. 9 The effect of the overall pressure ratio of the Brayton cycle on the inlet energy and power generation of the ORC

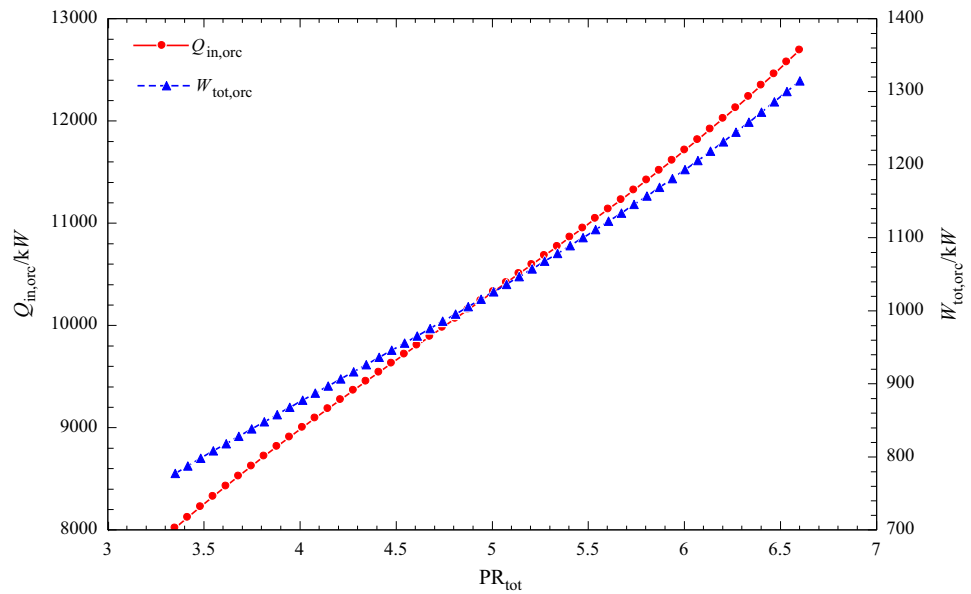
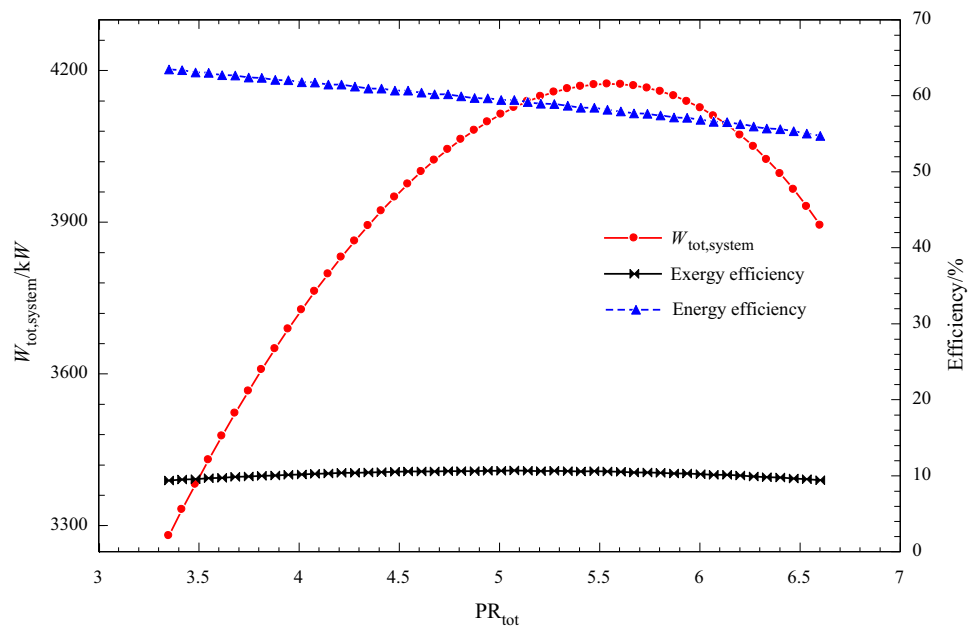


Fig. 10 Effect of the overall Brayton pressure ratio on the total power generation and the energy and exergy efficiencies of the system



Compressor pressure ratio analysis

This section examines the influence of the compressor pressure ratio as the total pressure ratio of the Brayton cycle on different parts of the system. An increase in the pressure ratio of the Brayton cycle first increases the specific work consumed by the compressor, as shown in Fig. 6. In addition, the specific work generated by the LP and HP turbines also increases due to the increase in the pressure ratio of each turbine. On the other hand, a pressure rise increases the compressor outlet temperature, leading to an increase in the temperature of Point 3 in the Brayton cycle. Therefore,

since the energy transferred from the inlet exhaust gas to the heat exchanger is constant, the flow rate increases. Finally, the total power generated by the Brayton cycle is highest at a pressure ratio of 5.2 owing to the increase in the power consumption of the compressor and the power generation of the turbines.

As mentioned previously, a rise in the compressor pressure ratio leads to an increase in the power generated by the turbines. As a result, the outlet temperature of the HP turbine decreases. This leads to an increase in the energy absorbed by the reheater. Hence, the energy entering the absorption chiller cycle decreases. Figure 7 depicts the impact of an

Fig. 11 The Pareto solution and the selection of the optimal point via the TOPSIS method

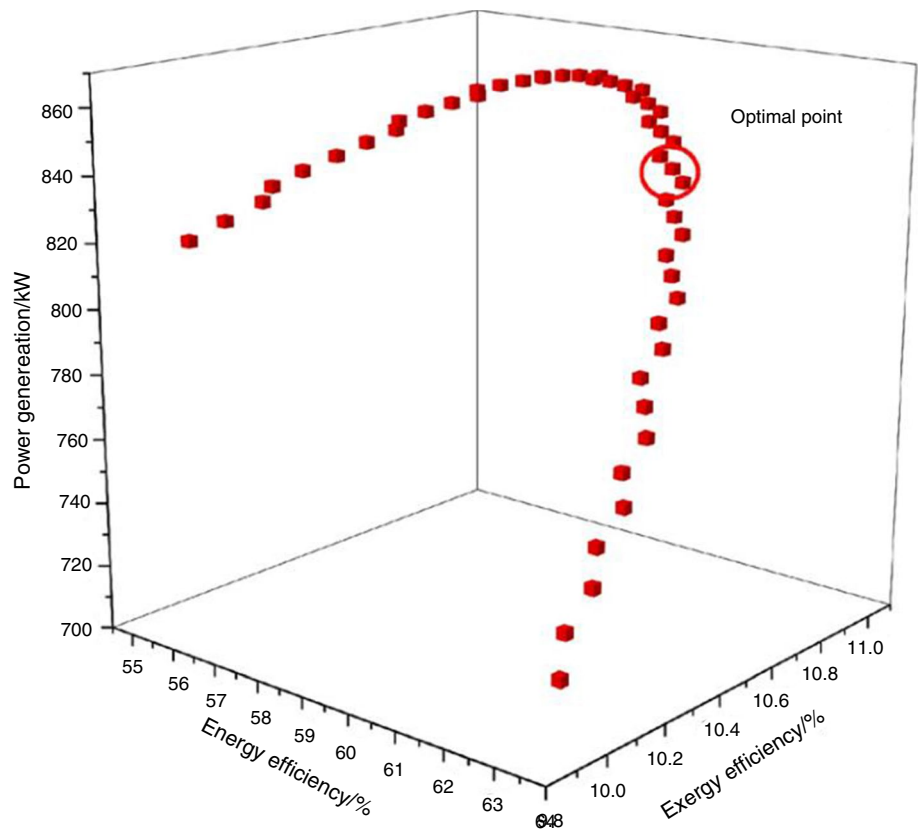
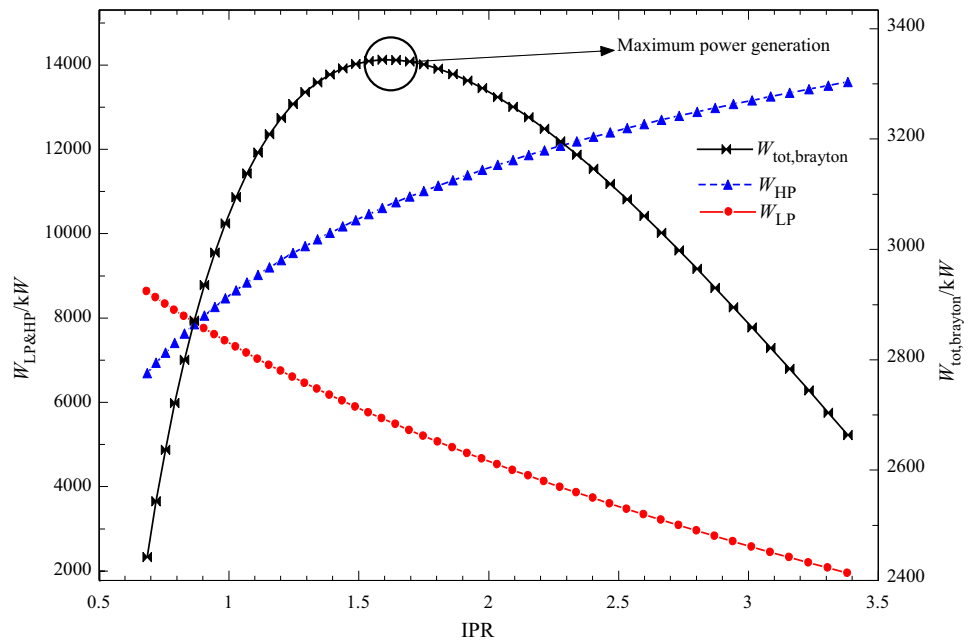


Fig. 12 The effect of an increase in the IPR on the power generated by the LP and HP turbines and the total power generated by the Brayton cycle



increase in the pressure ratio on the energy absorbed in the reheater and the absorption chiller.

The absorption chiller cycle is mostly dependent on the generator's inlet energy, which determines its generated cooling. The energy entering the absorption chiller

comes from the exhaust of the Brayton cycle. Accordingly, the energy inlet to the absorption chiller heat exchanger decreases with an increase in the pressure ratio of the Brayton cycle, as shown before. As a result, the cooling generated by the chiller also decreases. Nevertheless, the COP

Fig. 13 The effect of an increase in the IPR on the power generation of the ORC and cooling of the absorption chiller

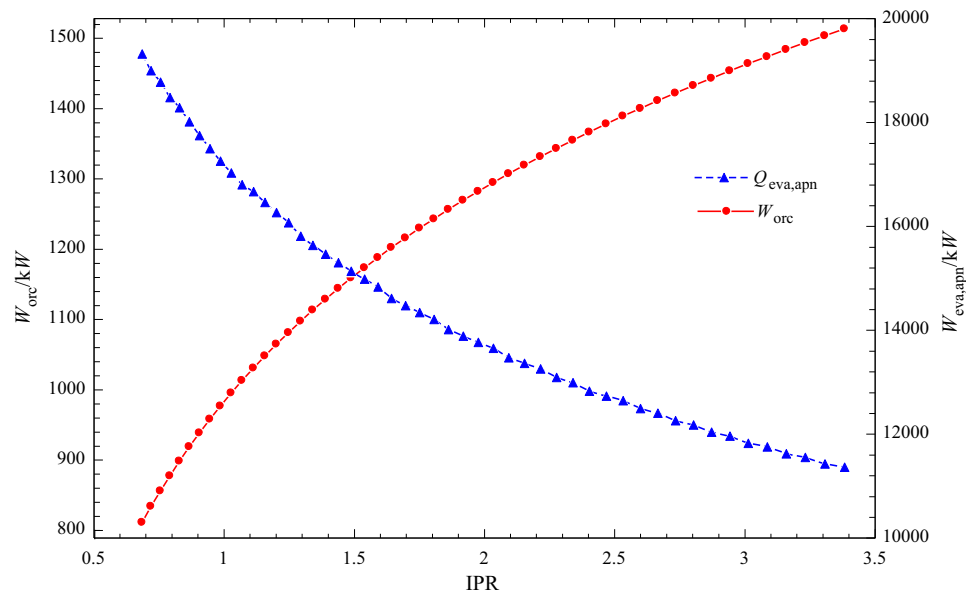
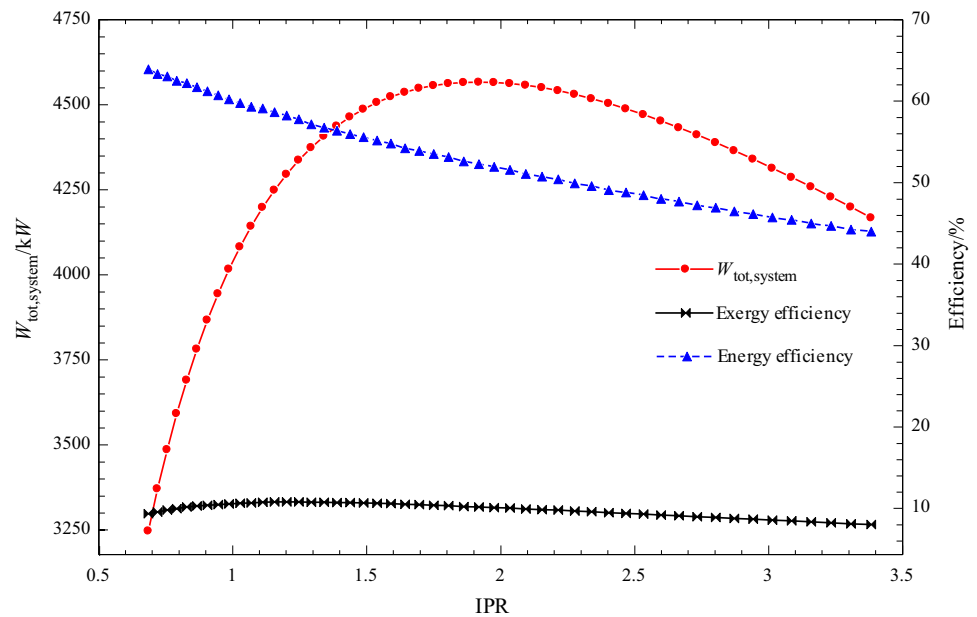


Fig. 14 The effect of the IPC on the total power generation and the exergy and energy efficiencies of the system

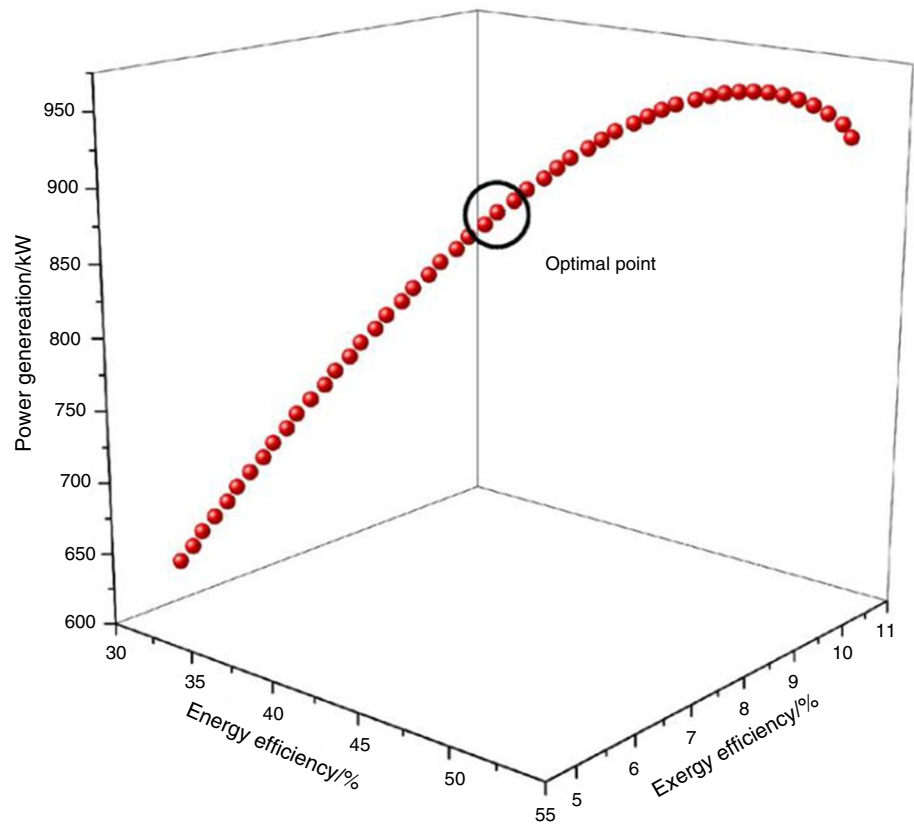


slightly changes due to its simultaneous dependence on the inlet energy and the generated cooling. Figure 8 shows the effect of an increase in the pressure ratio on the cooling generation and the COP of the absorption chiller.

An increase in the pressure ratio of the Brayton cycle reduces the LP turbine outlet temperature. On the other hand, the flow rate in the Brayton cycle increases, as previously stated. Finally, the energy entering the evaporator of the ORC increases, leading to an increase in the power generated by this cycle. Figure 9 shows the effect of the overall pressure ratio of the Brayton cycle on the inlet energy and power generation of the ORC.

Finally, the effects of changes in the pressure ratio on the overall energy and exergy efficiencies of the system were studied, and the results are shown in Fig. 10. As demonstrated previously, the power generated by the Brayton cycle was maximum at a pressure ratio of 5.2. On the other hand, the power generation in the ORC increases continuously with an increase in the pressure ratio. Moreover, the total power generated by the system is maximum at a pressure ratio of 5.4. On the other hand, the energy efficiency of the system has a decreasing trend due to the decrease in the cooling generated by the absorption chiller cycle. However, the exergy efficiency of the system is maximum at a pressure ratio of 4.73. The reason for the difference of this point from

Fig. 15 The Pareto solution and the selection of the optimal point via the TOPSIS method



the point of maximum generated power is the decreasing trend in the exergy efficiency of the absorption chiller.

Exergy is a thermodynamic term and refers to the maximum amount of useful work that can be obtained from a system in the process of achieving thermodynamic exchange. Exergy also means accessibility. Availability expresses the most work that can be extracted from the system. On the other hand, internal energy expresses the kinetic energy and potential of a micro-scale system. For example, on the scale of atoms and molecules, this energy can be described using their vibrational, rotational, and translational energies. Exergy can be defined as the amount of work that can be extracted from a system that has reached its thermodynamic equilibrium state through a reversible process. Also, there is a certain relationship between the entropy produced by a system and exergy. The production of entropy is equal to the amount of exergy lost. Entropy shows the inability of the system to produce work and exergy shows the ability of the system to produce work.

Finally, the optimal point of the system corresponding to the mentioned temperature conditions and working fluid was determined using the single-objective Pareto method and the TOPSIS technique based on power generation, energy efficiency, and exergy efficiency. Figure 11 shows the Pareto solution and the selection of the optimal

point via the TOPSIS method. The optimal pressure ratio in the TOPSIS solution is 4.942.

Determination of the turbine's pressure ratio in the Brayton cycle

In the previous section, the compressor pressure ratio, which is equal to the overall pressure ratio of the system, was examined using energy and exergy analysis, and its optimum value was determined. On the other hand, given that the system has two turbines in the Brayton cycle, the pressure ratio of each turbine can considerably affect the overall performance of the system. Accordingly, this section conducts an energy and exergy analysis in order to optimize the pressure ratio between the two turbines. To this end, first, the intermediation pressure ratio (IPR) parameter, which is obtained by dividing the pressure ratio of the HP turbine by that of the LP turbine, is introduced, as shown in Eq. (11).

$$\text{IPR} = \frac{\text{PR}_{\text{HP}}}{\text{PR}_{\text{LP}}} \quad (12)$$

In this equation, PR_{HP} is the pressure ratio of the HP turbine, while PR_{LP} is that of the LP turbine. As mentioned previously, the compressor pressure ratio is fixed, and only the pressure ratios of the LP and HP turbines vary. As a

Table 6 System optimization results for different heat sources and the suitable working fluid

Source temperature/°C	Working fluid	P1/kPa	PR _{tot}	IPR	$W_{\text{tot,sys}}/\text{kW}$	Energy efficiency/%	Exergy efficiency/%	$Q_{\text{cooling}}/\text{kW}$	COP
800	Air	100	12.48	2.614	860.2	58.26	10.81	3429	0.77
	He	100	4.942	1.389	4173	58.18	10.54	16,373	0.772
	O ₂	100	14.06		807.6	58.27	10.76	3266	0.7723
	CO ₂	100	48.88		877	58.3	11	3589	0.7722
	Xenon	100	5.714		127.7	57.72	10.82	495.8	0.7729
	N ₂	100	12.23		882.3	58.2	10.8	3502	0.7709
700	Air	100	9.33		624.7	57.56	8.16	2954	0.7707
	He	100	4.58		3063	57.54	8	14,268	0.7711
	O ₂	100	10.38		586.8	57.57	8.134	28.13	0.7717
	CO ₂	100	30.67		31.1	57.51	8.281	3061	0.7702
	Xenon	100	4.622		93.9	57.6	8.3	436	0.7738
	N ₂	100	9.157		640.7	57.52	8.148	3018	0.7702
600	Air	100	5.975		402.7	58.36	5.65	2568	0.7729
	He	100	3.416		1988	58.2	5.54	12,521	0.7718
	O ₂	100	6.622		378	58.08	5.614	2429	0.7729
	CO ₂	100	14.9		404	58.47	5.757	2641	0.7716
	Xenon	100			61.01	58.27	5.749	382.7	0.7712
	N ₂	100	5.871		413.1	58.36	5.647	2628	0.7727
500	Air	100	5.257		312.1	55.81	4.39	1913	0.7733
	He	100	2.885		1464	57.28	4.176	9839	0.7737
	O ₂	100	4.598		251.2	57.64	3.916	1927	0.7737
	CO ₂	100	9.898		273.3	56.9	4.061	2020	0.7735
	Xenon	100	2.882		44.71	57.31	4.325	300.9	0.7737
	N ₂	100	4.161		268	57.87	3.837	2095	0.7738
400	Air	100	4.551		279.6	57.15	4.048	1999	0.7736
	He	100	2.767		1392	57.79	4.015	10,012	0.7733
	O ₂	100	5.347		282.4	56.3	4.279	1845	0.7735
	CO ₂	100	10.94		288.1	56.29	4.228	1980	0.7737
	Xenon	100	2.757		42.36	57.89	4.14	306.6	0.7735
	N ₂	100	4.02		259.6	58.07	3.733	2111	0.772
300	Air	100	1.882		63.66	58.9	1.1	1026	0.7735
	He	100	1.577		328.4	58.5	1.1	5139	0.7724
	O ₂	100	1.941		59.95	58.65	1.108	959.5	0.7734
	CO ₂	100	2.6,2		62.47	58.24	1.14	988.6	0.7735
	Xenon	100		Not work					
	N ₂	100	1.871		65.34	58.94	1.1	1054	0.7735

result, the compressor power consumption remains constant. As seen before, an increase in the IPR indicates a rise in the pressure ratio of the HP turbine. Figure 12 displays the effect of an increase in the IPR on the power generated by the LP and HP turbines and the total power generated by the Brayton cycle. As seen in the figure, increasing the IPC increases the HP turbine power generation and decreases the LP turbine power generation. This is due to the difference between the inlet and outlet enthalpies of the turbines. Moreover, the total power generated in the Brayton cycle has a maximum point considering the

opposite power generation trends in the two turbines and the constant compressor power consumption. The maximum IPC is equal to 1.591.

In the next step, the effect of the IPC on the cooling generated by the absorption chiller and the power generated by the ORC is studied. Figure 13 depicts the effect of an increase in the IPR on the power generation of the ORC and cooling of the absorption chiller. As can be seen, the generated cooling is reduced with a rise in the IPR. This is due to the fact that an increase in the IPR reduces the HP turbine outlet temperature, hence increasing heat absorption

in the reheater. This, in turn, decreases the heat inlet to the absorption chiller, resulting in a fall in the generated cooling. On the other hand, the outlet temperature of the LP turbine increases due to a decrease in its pressure ratio. This results in an increase in the heat entering the ORC and a rise in its generated power.

Finally, the total power generated by the system and its energy and exergy efficiencies are studied to determine the optimal value of the IPR. Figure 14 depicts the effect of the IPC on the total power generation and the exergy and energy efficiencies of the system. As shown in the figure, the total power is maximum at $IPR = 1.918$. Also, the exergy efficiency is maximum at $IPR = 1.247$.

The energy and exergy studies indicated that the point of maximum exergy efficiency does not coincide with the point of maximum power generation. Accordingly, the Pareto solution was used to select the appropriate IPR value. In addition, the TOPSIS technique was employed to select the optimal point. Figure 15 shows the Pareto solution and the selection of the optimal point based on the TOPSIS technique. As a result, the optimal IPR value for the mentioned conditions was obtained to be 1.389. Therefore, the pressure ratios of the HP and LP turbines are, respectively, equal to 2.563 and 1.845.

The results showed that in the temperature range of 300 to 800 °C, helium gas is the most optimal option compared to other gases, because it has the highest amount of electricity production. For this reason, the optimization process is carried out for the best gas that is identified as helium.

Optimization

The previous section involved a study of the parameters affecting the system, namely the Brayton cycle initial pressure, the compressor pressure ratio, and the IPR. The results showed that changes in the parameters affect the various parts of the system differently. Thus, the Pareto solution was used for the optimization and the selection of suitable values. To this end, the compressor pressure ratio and the IPR were considered the variables, and the total power generation and the energy and exergy efficiencies were considered the objective functions. Next, the optimal values in the Pareto solution were calculated using the TOPSIS method. Table 6 presents the system parameters based on the optimal values obtained from the Pareto solution. The optimization results are shown for a temperature range of 300–800 °C. Based on the results, He gas led to the highest power generation at various temperatures. Therefore, if closed Brayton cycles can be used with He as the working fluid, considerably more power can be generated compared to the case of using air.

Conclusions

With the increase in world population and limited energy resources, countries have faced the problem of energy consumption. Crises that threaten countries and human societies, for this reason, methods that can maximize the performance of energy production systems have been the focus of researchers. The present research examined the use of waste heat in different industries for operating a hybrid closed Brayton cycle, ORC, and absorption chiller system. The temperature range used in this research covered all the heat sources and waste from 800 to 300 °C. In addition, HP and LP turbines were used to improve the system performance. The working fluids examined in this research were air, helium, oxygen, carbon dioxide, xenon, and nitrogen. The parameters affecting the performance of the system, namely the compressor inlet pressure, the compressor pressure ratio, and the IPR were investigated. The results indicated that an increase in the compressor pressure ratio does not significantly affect the system performance; hence, the inlet pressure was considered equal to 100 kPa. Moreover, the parameter study showed that changes in different parameters affect the various parts of the system differently, i.e., positively in some cases and adversely in others. As a result, the Pareto solution was used for optimization, and the TOPSIS technique was employed to obtain the optimal values. Based on the optimization results, using helium leads to a higher increase in power generation compared to other gases.

The summary of the results of this research can be stated as follows:

- Increasing the pressure of the compressor does not have a significant effect on the electricity consumption and the temperature of the working fluid due to the constant pressure ratio.
- Increasing the Brayton cycle pressure ratio first increases the work consumed by the compressor.
- The power produced by the Brayton cycle at a pressure ratio of 5.2 is the highest due to the increase in compressor power consumption and turbine power generation.
- The input energy to the heat exchanger of the absorption chiller decreases with the increase in the Brayton cycle pressure ratio, and as a result, the cooling created by the chiller also decreases.
- The results of the parametric study showed that the energy efficiency of the system is decreasing due to the reduction of the cooling produced by the absorption chiller cycle.
- The results of the parametric study showed that the exergy efficiency of the system has the maximum value at the pressure ratio of 4.73.

- Compressor pressure ratio and intermediation pressure ratio were considered as variables and total power production and energy efficiency and exergy were considered as objective functions.
- The optimization results were shown for the temperature range of 300–800 °C.
- The most optimal value of intermediation pressure ratio (IPR) was obtained after the optimization process of 1.389. Also, the most optimal value of pressure ratio of HP and LP turbines was reported as 2.563 and 1.845, respectively.

Funding Open access funding provided by Università degli Studi di Roma La Sapienza within the CRUI-CARE Agreement.

Open Access This article is licensed under a Creative Commons Attribution 4.0 International License, which permits use, sharing, adaptation, distribution and reproduction in any medium or format, as long as you give appropriate credit to the original author(s) and the source, provide a link to the Creative Commons licence, and indicate if changes were made. The images or other third party material in this article are included in the article's Creative Commons licence, unless indicated otherwise in a credit line to the material. If material is not included in the article's Creative Commons licence and your intended use is not permitted by statutory regulation or exceeds the permitted use, you will need to obtain permission directly from the copyright holder. To view a copy of this licence, visit <http://creativecommons.org/licenses/by/4.0/>.

References

1. Rahbar K, Mahmoud S, Al-dadah RK, Moazami N, Mirhadizadeh SA. Review of organic Rankine cycle for small-scale applications. *Energy Convers Manag.* 2017;134:135–55. <https://doi.org/10.1016/j.enconman.2016.12.023>.
2. Delovato N, Sundarnath K, Cvijovic L, Kota K, Kuravi S. A review of heat recovery applications for solar and geothermal power plants. *Renew Sustain Energy Rev.* 2019;114:109329. <https://doi.org/10.1016/j.rser.2019.109329>.
3. Kavvadias KC, Maroulis ZB. Multi-objective optimization of a trigeneration plant. *Energy Policy.* 2010;38(2):945–54. <https://doi.org/10.1016/j.enpol.2009.10.046>.
4. Deymi-Dashtebayaz M, Tayyeban E. Multi objective optimization of using the surplus low pressure steam from natural gas refinery in the thermal desalination process. *J Clean Prod.* 2019;238:117945. <https://doi.org/10.1016/j.jclepro.2019.117945>.
5. Huang W, Wang J, Xia J, Zhao P, Dai Y. Performance analysis and optimization of a combined cooling and power system using low boiling point working fluid driven by engine waste heat. *Energy Convers Manag.* 2019;180:962–76. <https://doi.org/10.1016/j.enconman.2018.11.041>.
6. Ma Y, Zhang X, Liu M, Yan J, Liu J. Proposal and assessment of a novel supercritical CO₂ Brayton cycle integrated with LiBr absorption chiller for concentrated solar power applications. *Energy.* 2018. <https://doi.org/10.1016/j.energy.2018.01.155>.
7. Amiri Rad E, Mohammadi S, Tayyeban E. Simultaneous optimization of working fluid and boiler pressure in an organic Rankine cycle for different heat source temperatures. *Energy.* 2020;194:116856. <https://doi.org/10.1016/j.energy.2019.116856>.
8. Sharaf Eldean MA, Soliman AM. A novel study of using oil refinery plants waste gases for thermal desalination and electric power generation: energy, exergy and cost evaluations. *Appl Energy.* 2017;195:453–77. <https://doi.org/10.1016/j.apenergy.2017.03.052>.
9. Mahmoudi A, Fazli M, Morad MR. A recent review of waste heat recovery by Organic Rankine Cycle. *Appl Therm Eng.* 2018. <https://doi.org/10.1016/j.applthermaleng.2018.07.136>.
10. Rovira A, Muñoz M, Sánchez C, Barbero R. Advanced thermodynamic cycles for finite heat sources: proposals for closed and open heat sources applications. *Appl Therm Eng.* 2020;167:114805. <https://doi.org/10.1016/j.applthermaleng.2019.114805>.
11. Khalil KM, Mahmoud S, Al-dadah RK. Development of innovative non-repeated annular area dual stage small-scale nitrogen axial turbine for hybrid open-closed Rankine cycle. *Energy Convers Manag.* 2018;164(February):157–74. <https://doi.org/10.1016/j.enconman.2018.02.088>.
12. Meas MR. Thermodynamic design optimisation of an open air recuperative twin-shaft solar thermal Brayton cycle with combined or exclusive reheating and intercooling. *Energy Convers Manag.* 2017;148:770–84. <https://doi.org/10.1016/j.enconman.2017.06.043>.
13. Kumar O, Kaushik SC. Thermo-economic evaluation and optimization of a Brayton–Rankine–Kalina combined triple power cycle. *Energy Convers Manag.* 2013;71:32–42. <https://doi.org/10.1016/j.enconman.2013.03.017>.
14. Naserian MM, Farahat S, Sarhaddi F. New exergy analysis of a regenerative closed Brayton cycle. *Energy Convers Manag.* 2017;134:116–24. <https://doi.org/10.1016/j.enconman.2016.12.020>.
15. Alali E, Al-shboul KF. Annals of nuclear energy performance analysis of the closed Brayton power cycle in a small-scale pebble bed gas cooled reactor using different working fluids. *Ann Nucl Energy.* 2018;121:316–23. <https://doi.org/10.1016/j.anucene.2018.07.040>.
16. Romano LFR, Ribeiro GB. Cold-side temperature optimization of a recuperated closed Brayton cycle for space power generation. *Therm Sci Eng Prog.* 2020;17:100498. <https://doi.org/10.1016/j.tsep.2020.100498>.
17. Xia J, Wang J, Lou J, Zhao P, Dai Y. Thermo-economic analysis and optimization of a combined cooling and power (CCP) system for engine waste heat recovery. *Energy Convers Manag.* 2016;128:303–16. <https://doi.org/10.1016/j.enconman.2016.09.086>.
18. Reza H, Pourrahmani H. Multi-objective optimization and exergo-economic analysis of a continuous solar-driven system with PCM for power, cooling and freshwater production. *Energy Convers Manag.* 2020;211:112761. <https://doi.org/10.1016/j.enconman.2020.112761>.
19. Feng Y, Du Z, Shreka M, Zhu Y, Zhou S, Zhang W. Thermodynamic analysis and performance optimization of the supercritical carbon dioxide Brayton cycle combined with the Kalina cycle for waste heat recovery from a marine low-speed diesel engine. *Energy Convers Manag.* 2020;206:112483. <https://doi.org/10.1016/j.enconman.2020.112483>.
20. Ahmadi P, Dincer I, Rosen MA. Exergo-environmental analysis of an integrated organic Rankine cycle for trigeneration. *Energy Convers Manag.* 2012;64:447–53. <https://doi.org/10.1016/j.enconman.2012.06.001>.
21. Miao H, Wang Z, Niu Y. Key issues and cooling performance comparison of different closed Brayton cycle based cooling systems for scramjet. *Appl Therm Eng.* 2020;179:115751. <https://doi.org/10.1016/j.applthermaleng.2020.115751>.

22. Sachdeva J, Singh O. Thermodynamic analysis of solar powered triple combined brayton, rankine and organic Rankine Cycle for carbon free power. *Renew Energy*. 2019. <https://doi.org/10.1016/j.renene.2019.02.128>.
23. Abrosimov KA, Baccioli A, Bischi A. Techno-economic analysis of combined inverted Brayton: Organic Rankine cycle for high-temperature waste heat recovery. *Energy Convers Manag*. 2020;207: 112336. <https://doi.org/10.1016/j.enconman.2019.112336>.
24. Mohammadi S, Rad EA. Evaluation of a heat recovery steam cycle based on energy, exergy, environmental and economic analyses. *Int J Exergy*. 2020;31(3):268–86. <https://doi.org/10.1504/IJEX.2020.106455>.
25. Tayyeban E, Deymi-Dashtebayaz M, Gholizadeh M. Investigation of a new heat recovery system for simultaneously producing power, cooling and distillate water. *Energy*. 2021;229: 120775. <https://doi.org/10.1016/j.energy.2021.120775>.
26. Liu H, Chi Z, Zang S. Optimization of a closed Brayton cycle for space power systems. *Appl Therm Eng*. 2020;179:115611.
27. Kim S, Kima MS, Kim M. Parametric study and optimization of closed Brayton power cycle considering the charge amount of working fluid. *Energy*. 2020;198:117353.
28. Zhang B, Chen Y, Wang Z, Shakibi H. Thermodynamic, environmental, and optimization of a new power generation system driven by a gas turbine cycle. *Energy Rep*. 2020;6:2531–48.
29. Musharavati F, et al. Multi-objective optimization of a biomass gasification to generate electricity and desalinated water using Grey Wolf Optimizer and artificial neural network. *Chemosphere*. 2022;287: 131980.
30. Khanmohammadi S, et al. Thermodynamic modeling and multi-objective optimization of a solar-driven multi-generation system producing power and water. *Desalination*. 2023;545: 116158.
31. Ding G-C, et al. Technical assessment of multi-generation energy system driven by integrated renewable energy sources: energetic, exergetic and optimization approaches. *Fuel*. 2023;331: 125689.
32. Colakoglu M, Durmayaz A. Energy, exergy, economic and emission saving analysis and multiobjective optimization of a new multi-generation system based on a solar tower with triple combined power cycle. *Sustain Energy Technol Assess*. 2022;52: 102289.
33. Alirahmi SM, et al. Development and multi-criteria optimization of a solar thermal power plant integrated with PEM electrolyzer and thermoelectric generator. *Int J Hydrog Energy*. 2022;47(57):23919–34.
34. Asadi R, et al. Optimisation of combined cooling, heating and power (CCHP) systems incorporating the solar and geothermal energy: a review study. *Int J Ambient Energy*. 2022;43(1):42–60.
35. Assareh E, et al. An extensive thermo-economic evaluation and optimization of an integrated system empowered by solar-wind-ocean energy converter for electricity generation—case study: Bandar Abbas, Iran. *Therm Sci Eng Prog*. 2021;25: 100965.
36. Assareh E, et al. Thermodynamic assessment of a cogeneration system with CSP Driven-Brayton and Rankine cycles for electric power and hydrogen production in the framework of the energy and water nexus. *Energy Nexus*. 2022;5: 100031.
37. Assareh E, et al. Optimization of geothermal- and solar-driven clean electricity and hydrogen production multi-generation systems to address the energy nexus. *Energy Nexus*. 2022;5: 100043.
38. Azizimehr B, et al. Thermoeconomic analysis and optimization of a solar micro CCHP by using TLBO algorithm for domestic application. *Energy Sources Part A Recovery Util Environ Eff*. 2020;42(14):1747–61.
39. Dezhdar A, et al. A transient model for clean electricity generation using Solar energy and ocean thermal energy conversion (OTEC): case study: Karkheh dam—southwest Iran. *Energy Nexus*. 2023;9: 100176.
40. Shakibi H, et al. Exergoeconomic and optimization study of a solar and wind-driven plant employing machine learning approaches; a case study of Las Vegas city. *J Clean Prod*. 2023;385: 135529.
41. Rejeb O, et al. Innovative integrated solar powered polygeneration system for green hydrogen, oxygen, electricity and heat production. *Energy Convers Manag*. 2022;269: 116073.
42. Shakibi H, et al. Using machine learning approaches to model and optimize a combined solar/natural gas-based power and freshwater cogeneration system. *Appl Energy*. 2023;333: 120607.
43. Behrang MA, et al. Assessment of electricity demand in iran's industrial sector using different intelligent optimization techniqueS. *Appl Artif Intell*. 2011;25(4):292–304.
44. Nedaei M, et al. A comprehensive evaluation of the wind resource characteristics to investigate the short term penetration of regional wind power based on different probability statistical methods. *Renew Energy*. 2018;128:362–74.
45. Akhouni M, et al. Parametric study and optimization of the pre-cooled Linde-Hampson (PCLH) cycle for six different gases based on energy and exergy analysis. *Chem Pap*. 2023;77(9):5343–56.
46. Amiri Rad E, et al. Simultaneous optimization of working fluid and boiler pressure in an organic Rankine cycle for different heat source temperatures. *Energy*. 2020;194: 116856.
47. Dadpour D, et al. Proposing a new method for waste heat recovery from the internal combustion engine for the double-effect direct-fired absorption chiller. *Appl Therm Eng*. 2022;216: 119114.
48. Dadpour D, et al. Multi objective optimization and 3E analyses of a novel supercritical/transcritical CO₂ waste heat recovery from a ship exhaust. *Energy*. 2023;278: 127843.
49. Dadpour D, et al. Vehicle refrigeration modification using an ejector: optimization and exergoeconomic analysis. *J Taiwan Inst Chem Eng*. 2023;148: 104875.
50. Ghorbani S, et al. Parametric investigation and performance optimization of a MED-TVC desalination system based on 1-D ejector modeling. *Energy Convers Manag*. 2023;288: 117131.
51. Tayyeban E, et al. Multi objective optimization of MSF and MSF-TVC desalination systems with using the surplus low-pressure steam (an energy, exergy and economic analysis). *Comput Chem Eng*. 2022;160: 107708.
52. Norani M, Deymi-Dashtebayaz M, Gholizadeh M et al. Modeling and multi-objective optimization of a combined cooling, fresh water and power system for gas turbine waste heat recovery, 16 August 2022, PREPRINT (Version 1) available at Research Square <https://doi.org/10.21203/rs.3.rs-1948733/v1>
53. Tavana M, Deymi-Dashtebayaz M, Dadpour D, Mohseni-Gharyehsafa B. Realistic energy, exergy, and exergoeconomic (3E) characterization of a steam power plant: multi-criteria optimization case study of mashhad tous power plant. *Water*. 2023;15:3039. <https://doi.org/10.3390/w15173039>.
54. Gholizadeh M, Deymi-Dashtebayaz M, Mehri A, et al. Experimental evaluation and optimization of the anaerobic digestibility of two new desert weeds for biogas production. *Biomass Conv Bioref*. 2022. <https://doi.org/10.1007/s13399-022-02884-5>.
55. Farhadi F, Deymi-Dashtebayaz M, Tayyeban E. Studying a multi-stage flash brine recirculation (MSF-BR) system based on energy. *Exergy Exergoeconomic Anal Water*. 2022;14:3108. <https://doi.org/10.3390/w14193108>.
56. Soltani M, Nabat MH, Razmi AR, Dusseault MB, Nathwani J. A comparative study between ORC and Kalina based waste heat recovery cycles applied to a green compressed air energy storage

- (CAES) system. *Energy Convers Manag.* 2020;222: 113203. <https://doi.org/10.1016/j.enconman.2020.113203>.
57. Razmi A, Soltani M, Tayefeh M, Torabi M, Dusseault MB. Thermodynamic analysis of compressed air energy storage (CAES) hybridized with a multi-effect desalination (MED) system. *Energy Convers Manag.* 2019;199: 112047. <https://doi.org/10.1016/j.enconman.2019.112047>.
 58. Amiri Rad E, Mohammadi S. Energetic and exergetic optimized Rankine cycle for waste heat recovery in a cement factory. *Appl Therm Eng.* 2018;132:410–22. <https://doi.org/10.1016/j.applthermaleng.2017.12.076>.
 59. Liu H, et al. Optimization of a closed Brayton cycle for space power systems. *Appl Therm Eng.* 2020;179: 115611.
 60. Liu Z, et al. Performance assessment of closed Brayton cycle-organic Rankine cycle lunar base energy system: thermodynamic analysis, multi-objective optimization. *Energy.* 2023;278: 127936.
 61. Dincer I, Ozturk M. Chapter 1: Thermodynamic fundamentals. In: Dincer I, Ozturk M, editors. *Geothermal energy systems*. Elsevier; 2021. p. 1–30.
 62. Dincer I, Rosen MA. Chapter 1: Thermodynamic fundamentals. In: Dincer I, Rosen MA, editors. *Exergy*. 3rd ed. Elsevier; 2021. p. 1–22.
 63. Lewis M. Chapter 26: Thermodynamic charts and refrigeration. In: Lewis M, editor. *Food process engineering principles and data*. Woodhead Publishing; 2023. p. 237–45.
 64. Imamović B, et al. Comprehensive fuzzy logic coefficient of performance of absorption cooling system. *Expert Syst Appl.* 2022;190: 116185.
 65. Nilavarasi K, Ponmurugan M. Optimized coefficient of performance of power law dissipative Carnot like refrigerator. *Physica A.* 2022;590: 126700.
 66. Rafiee SE. Experimental and thermo-dynamical analysis of fully turbulent gas flows in vortex tube-fluid, temperature and power separations, isentropic efficiency, coefficient of performance (COP). *Int Commun Heat Mass Transfer.* 2022;138: 106296.
 67. Wang Y, et al. BMW-TOPSIS: a generalized TOPSIS model based on three-way decision. *Inf Sci.* 2022;607:799–818.
 68. Zhang K, Dai J. A novel TOPSIS method with decision-theoretic rough fuzzy sets. *Inf Sci.* 2022;608:1221–44.

Publisher's Note Springer Nature remains neutral with regard to jurisdictional claims in published maps and institutional affiliations.